

University of California
Santa Barbara

Synchronization in Pulse-Coupled Oscillator With Delays and Mixed Excitatory/Inhibitory Coupling

A Thesis submitted in partial satisfaction
of the requirements for the degree

Master of Science
in
Mechanical Engineering

by

Deepti Kannapan

Committee in charge:

Francesco Bullo, Chair
Jeff Moehlis
Brad Paden

June 2015

The Thesis of Deepti Kannapan is approved.

Jeff Moehlis

Brad Paden

Francesco Bullo, Committee Chair

June 2015

Synchronization in Pulse-Coupled Oscillator
With Delays and Mixed Excitatory/Inhibitory Coupling

Copyright © 2015

by

Deepti Kannapan

Acknowledgements

I would like to acknowledge my advisor Francesco Bullo for setting me down the road that led to the work in this thesis, and for his enthusiastic support along the way. I would like to thank my other committee members, Jeff Moehlis and Brad Paden, for their interest and advice, and the UCSB Department of Mechanical Engineering for a thorough engineering education, academic resources and administrative support. I would like to thank my friends and colleagues, Pushkarini Agharkar and Jonathan Epperlein, for being invested in and contributing to my well-being. And lastly and most importantly, Mom, Dad and Pree for being their awesome, encouraging selves.

Abstract

Synchronization in Pulse-Coupled Oscillator With Delays and Mixed Excitatory/Inhibitory Coupling

by

Deepti Kannapan

Pulse coupled oscillator (PCO) networks consist of oscillators that send pulses to their in-neighbors on the network, as defined by the *sensing digraph*. The neighbors update their phase when they receive the pulse, depending on their current phase and the pulse strength. This mechanism causes the oscillators to synchronize for some values of their initial phases, and to converge to a fixed phase difference for others. The synchronizing behavior due to pulse coupling has been observed in nature: fireflies tend to flash in unison, neurons and cardiac cells synchronize their firing with their neighboring cells by this mechanism.

There has been recent interest in developing algorithms based on PCO networks to synchronize the clocks for distributed sensing and robotic applications. PCO networks whose sensing digraphs are strongly connected have been modeled extensively, in the presence and absence of delays in the transmissions of pulses, using analytical and numerical approaches.

We model a PCO network whose sensing digraph is not necessarily strongly connected but satisfies the weaker condition of having a globally reachable node. We propose a simple model of PCO networks with identical frequencies, based on the approach used in the study of distributed consensus. We model the discrete dynamics of the network as a linear time-varying (LTV) system. We use the row-stochastic property of the weighted adjacency matrices that characterize the LTV system, to derive sufficient conditions for synchrony. Arbitrary delays in the pulse-transmission

are modeled as disturbances. Synchrony may not be reached exactly in the presence of delays, and error that remains in the phases in the steady state is proportional to the maximum delay.

Further, we observe the convergence to be exponential if sampled over a sufficiently large number of receptions, and estimate the rate of convergence based on the properties of the digraph. We also estimate the basin of attraction of the synchronized solution. We illustrate these results with numerical examples.

Contents

Abstract	v
List of Figures	viii
List of Tables	ix
1 Introduction	1
1.1 Problem Description	1
1.2 Motivation	2
1.3 PCO Network Models in Literature	3
1.4 Contribution	4
1.5 Organization of this Thesis	6
2 Pulse-Coupled Oscillator Network Model	8
2.1 System Equations	8
2.2 Geometry of the Phase Vector	10
2.3 Synchrony	10
2.4 Definitions	10
3 Estimating Durations Between Pulses	13
4 Synchronization with No Delays	17
5 Synchronization with Delays	25
6 Examples and Numerical Simulations	37
7 Conclusion	41
Appendix A: Simulation Program	43
Bibliography	54

List of Figures

2.1	Phase of an oscillator, $\phi_4(t)$	9
2.2	An example of a sensing digraph, \mathcal{G}	9
2.3	Two examples of reception digraphs consistent with the sensing digraph in Figure 2.2, where oscillator 2 receives a pulse from oscillator 1 (on the left) and where oscillator 3 receives a pulse from oscillator 4 (on the right).	12
4.1	The coordinate transformation from $\phi(t)$ to $\tilde{\phi}(t)$ in the rotating coordinate frame. The origin of rotating coordinate frame is at a counterclockwise distance of $c(t)$ from the origin of the fixed coordinate frame.	19
5.1	An example of a modified reception digraph $\tilde{\mathcal{G}}_p$, consistent with the reception digraph on the left in Figure 2.3, where oscillator 2 receives a pulse from oscillator 1 at t_p , and where two receptions have occurred in the duration $]t_p - \tau_{21}, t_p[$	36
6.1	A magnification of the graph in Table 6.1 for example 2.	40

List of Tables

- 1.1 A summary of the literature on the six kinds of PCO networks. . . . 5
- 6.1 Example simulation results. All the simulations use $h = .06$ 39

1 Introduction

1.1 Problem Description

Coupled oscillator networks consist of oscillators (1D systems that would each be periodic in isolation). The dynamics of an oscillator is coupled to the dynamics of other oscillators that it can sense, that is, its out-neighbors in the sensing digraph (‘network’). The coupling could be discrete or continuous, and are referred to as pulse coupling and diffusive coupling respectively [16]. In networks of pulse-coupled oscillators (PCO), an oscillator sends a pulse (or ‘fires’) to its in-neighbors on the sensing digraph every time it completes an oscillation. An oscillator experiences a discrete jump in its phase on reception of the pulse. The phase jump could be forward or backward and depends on its current phase. It is defined by the *phase response curve* (see [20]). The network is a hybrid system, since its state, comprising the phases of all the oscillators, varies continuously with time except when any oscillator receives a pulse.

PCO network models have been studied extensively since they have been useful both for modeling naturally occurring phenomena and for technological applications. The oscillators are often assumed to be identical or nearly identical. Two behaviors that are exhibited by the networks have been studied extensively: reaching *synchrony* (where all the oscillators have the same phase) or an *asynchronous* state [26] (where the oscillators have distinct phases whose separation remains constant with time), from arbitrary initial phases. Both of these types of final conditions are periodic. We refer to the process in which the separation between phases converges to a constant value near zero as *synchronization*.

We broadly classify PCO network models in the literature according to the type of coupling (**excitatory**, **inhibitory** or **mixed**) and according to the presence or absence of **delay** in the transmission of pulses. Excitatory coupling refers to coupling

where an oscillator experiences an increase in phase whenever it receives a pulse. Inhibitory coupling refers to coupling where an oscillator experiences a decrease in phase whenever it receives a pulse. Mixed excitatory/inhibitory coupling (referred to in [20] as *advance-delay* coupling) refers to coupling where pulses either cause the phase to jump forward (‘advance’) or backward (‘delay’) depending on the current value of the phase. *Delay* in the transmission of pulses refers to the duration between the transmission of a pulse (when an oscillator fires) and the reception of the pulse by an in-neighbor of the sending oscillator. (‘Delay’ will be used to refer only to transmission delay from now on.) By these two criteria, there are six types of PCO networks. Additionally, for each type of network, the behavior differs based on the type of sensing digraph. The most common types that are studied are **all-to-all** (complete graph with no self loops), and **graphs that satisfy the weaker condition of being strongly connected or strongly rooted**.

1.2 Motivation

Occurrences in Nature One of the first phenomena that sparked interest in PCO networks was the synchronization of South Asian fireflies in their lighting patterns [1], with the flashes of each firefly acting as the signal to the the others. Another natural phenomenon, the self-synchronization of the pacemaker cells of the heart, was studied by Peskin in [21]. Both of these phenomena have been modeled as PCO networks with excitatory coupling and no delay. Lastly, the electrical signals of neurons have been modeled extensively as PCO networks with inhibitory coupling and delay [24, 12, 3, 11].

Technological Applications PCO network-based algorithms have been used for clock synchronization for wireless transceivers [18], in cellular mobile radio [27], robotics [4, 22, 30], wireless sensor networks [10, 9, 6, 23, 28], scheduling [8] and

management [5].

Modified Versions of PCO Networks Modified algorithms for improved synchronization properties have been proposed for improved synchronization properties for technological applications. A *refractory period* is a period during which an oscillator becomes unable to receive signals, right after it fires. It is sometimes incorporated into inhibitory systems to eliminate ‘echo’ effects [15, 13, 19]. *Self adjustment* is an instantaneous self-coupling during firing that is sometimes introduced to enable the system to get closer to synchrony [13].

1.3 PCO Network Models in Literature

The behavior of PCO networks has been investigated for the three types of couplings mentioned above, both with and without delays, as summarized in Table 1.1. In most cases, the sensing digraph is assumed to be strongly connected though sometimes the type of sensing digraph is further restricted to simplify the proof.

Excitatory Couplings PCO networks with **excitatory coupling and no delay** reach synchrony from any initial condition (excluding a set of Lebesgue measure 0). This was proved analytically for the case of all-to-all coupling by Mirollo and Strogatz in [17]. Numerical simulations in the same paper indicate that any strongly connected sensing digraph would also reach synchrony (albeit slower), though this has not been proved.

Interestingly, the behavior of the system completely changes on the introduction of even the smallest **delay**. The system reaches the asynchronous state from all initial conditions and not synchrony, as shown in [7] and [25]. In [29] it is proved that synchrony in this case is in fact impossible. This makes excitatory couplings unsuitable for a practical synchronization applications, since small delays are inevitable.

Inhibitory Couplings For PCO networks with **inhibitory coupling and no delay**, both synchrony and asynchronous states are possible, depending on the initial conditions. In [14], it is proved that in the all-to-all case, synchrony is reached irrespective of the initial conditions. However, in general, asynchronous states can occur as described in [12].

PCO networks with **inhibitory coupling and delay** also exhibit a coexistence of the asynchronous state and synchrony, depending on the initial conditions as described in [26]. In [25] it is proved that the synchronous state is locally stable if the delay is greater than some threshold. There is no proof however for arbitrarily small delays.

Mixed Excitatory/Inhibitory Couplings For PCO networks with mixed excitatory/inhibitory couplings, the behavior is not known in general. For a **specific** choice of phase response curve, it is shown in [20] that, in the absence of delays, the system reaches synchrony for all initial conditions if the coupling strength is above some threshold. If the coupling strength is below the threshold, it synchronizes only from initial conditions of phases contained within an angle of π .

For the systems with delays, it is proved in [19] that similar behavior to the above occurs for the special case of undirected cycle graphs. For directed cycle graphs, a refractory period has to be added to one of the oscillators to ensure that exact synchrony is reached.

1.4 Contribution

The contributions of this thesis are as follows. We study the timing behavior of the firings and receptions in the PCO network, and derive bounds on the durations between successive firings of an oscillator, and successive receptions along an edge. We propose a simple model of a PCO network with delays and mixed excita-

Table 1.1: A summary of the literature on the six kinds of PCO networks.

	Excitatory coupling	Inhibitory coupling	Mixed excitatory/inhibitory coupling
With no delays	[17]: Sufficient conditions for all-to-all PCOs to asymptotically synchronize from almost all initial conditions.	[12], [14]: Coexistence of synchrony and asynchronous states. Sufficient conditions for all-to-all PCOs to asymptotically synchronize from all initial conditions.	[20]: Sufficient conditions for strongly connected PCOs to asymptotically synchronize from all initial conditions if the coupling strength is above a threshold, and for initial conditions within an angle of $\frac{\pi}{2}$ otherwise.
With delays	[29], [7], [25]: Asynchronous states are reached from all initial conditions and synchrony is impossible.	[26], [25]: Coexistence of synchrony and asynchronous states. Synchrony is proven stable if the delay is sufficiently large.	[19]: Similar behavior to the above for the special cases of undirected cycle graphs, and of directed cycle graphs with refractory periods to ensure exact synchrony.

tory/inhibitory coupling as a linear time-varying (LTV) system, based on the timing behavior.

We then derive sufficient conditions on the sensing digraph for the PCO network to synchronize exactly if the delays are all zero, or to synchronize approximately, if non-zero delays are present. Using techniques commonly used to analyze distributed consensus problems, we show that synchronization is possible on graphs that are not necessarily strongly connected but satisfy the weaker condition of having a globally reachable node.

We also show that the convergence is exponential, in the sense that the separation between the phases converges exponentially to a constant value (if delays are present), or to zero (if no delays are present), when sampled over a large enough duration. We estimate the rate at which convergence occurs from the out-degrees and other properties of the sensing digraph. In situations where exact synchronization does not occur, we estimate the error between the oscillator phases that remains in the final asynchronous state, and we estimate the basin of attraction of the final state.

1.5 Organization of this Thesis

The rest of this thesis is organized as follows. In Section 2, we describe the system equations of the PCO network and define the functions and parameters that are used in the subsequent sections. In Section 3, we derive basic results on how many pulses an oscillator can receive in a duration of known length. In Section 4, we assume that no delays are present, and rewrite the system equations of the PCO network as an LTV system and derive sufficient conditions for the network to synchronize exactly. We also estimate the rate at which the error between the oscillators exponentially converges to zero. In Section 5, we rewrite the system equations of the PCO network as an LTV system with disturbances proportional to the delays, and derive sufficient conditions for the error between the oscillators to

converge exponentially. We also estimate the final value of this error and estimate the rate at which the error converges. In Section 6, we present numerical simulations of the PCO network that illustrate the behaviors described in Sections 4 and 5 for specific examples. Lastly, in Section 7, we describe how the contributions of this thesis may be relevant to future work.

2 Pulse-Coupled Oscillator Network Model

We consider a PCO network system with delays and with mixed excitatory/inhibitory coupling similar to that described in [20], that is, where the phase of the oscillator jumps toward 0 (or 1, whichever is nearer), by a distance proportional to the arc from its phase to 0 (or 1), whenever it receives a pulse. We study the case with delays, and hence this thesis addresses the problem in the second row, second column of 1.1.

2.1 System Equations

The *PCO network* consists consists of N oscillators. The phase of each oscillator $i \in \{1, \dots, N\}$ evolves on a circle of unit circumference. The phase, denoted by $\phi_i(t) \in [0, 1[$, is the length of the counter-clockwise arc from the positive horizontal axis to the state of the oscillator, as shown in Figure 2.1. In what follows we regard the circle of unit circumference equivalent to the interval $[0, 1[$. Each oscillator obeys a hybrid dynamics with continuous-time evolution on the circle, discrete jumps due to pulses, and a discrete *reset* to 0 on firing, when the phase reaches 1. The continuous-time dynamics is described by

$$\dot{\phi}_i(t) = 1. \tag{2.1}$$

The discrete-time dynamics is described as follows:

- (i) when the phase ϕ_i reaches 1, it is reset to 0 and the oscillator i sends a pulse to each of its in-neighbors in a *sensing digraph* \mathcal{G} ;
- (ii) assuming a pulse is sent from oscillator i at time t , it is received by its in-neighbor j at time $t + \tau_{ij}$, where τ_{ij} is a non-negative *delay*;
- (iii) assuming the oscillator i receives a pulse at time t , it jumps to a new phase

$\phi_i(t^+)$ as follows:

$$\phi_i(t^+) = \begin{cases} \phi_i(t) - h\phi_i(t), & \text{if } \phi_i(t) \in [0, \frac{1}{2}[, \\ \phi_i(t) + h(1 - \phi_i(t)), & \text{if } \phi_i(t) \in [\frac{1}{2}, 1], \end{cases} \quad (2.2)$$

where $h \in (0, 1)$ is a *pulse strength*.

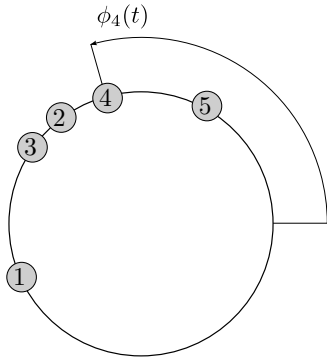


Figure 2.1: Phase of an oscillator, $\phi_4(t)$

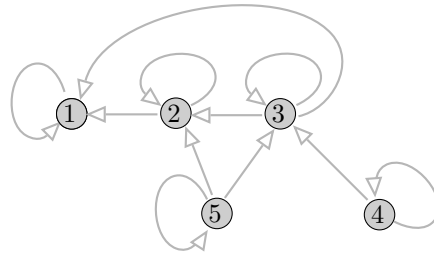


Figure 2.2: An example of a sensing digraph, \mathcal{G} .

2.2 Geometry of the Phase Vector

The phase of each oscillator evolves on a circle of unit circumference. The vector of the phases of the N oscillators exists in the N -torus which we will denote as \mathbb{T}^N and consists of N copies of the circle of unit circumference.

Distances The *clockwise arc-length* $\text{dist}_c(\phi_i, \phi_j)$ is the length of the clockwise arc from ϕ_i and ϕ_j . The *counterclockwise arc-length* $\text{dist}_{cc}(\phi_i, \phi_j)$ is the length of the counter-clockwise arc from ϕ_i and ϕ_j . The *geodesic distance* between ϕ_i and ϕ_j is the minimum between clockwise and counterclockwise arc-lengths and is denoted by $\text{dist}(\phi_i, \phi_j)$. In the parametrization described above: $\text{dist}_{cc}(\phi_i, \phi_j) = (\phi_j - \phi_i) \bmod 1$, $\text{dist}_c(\phi_i, \phi_j) = (\phi_i - \phi_j) \bmod 1$ $\text{dist}(\phi_i, \phi_j) = \min \{ \text{dist}_c(\phi_i, \phi_j), \text{dist}_{cc}(\phi_i, \phi_j) \}$.

Arc Subsets of the N -Torus Given a length $\gamma \in [0, 1]$, the arc subset $\Gamma(\gamma) \subseteq \mathbb{T}^N$ is the set of N -tuples (ϕ_1, \dots, ϕ_N) such that there exists an arc of length *strictly* less than γ containing all ϕ_1, \dots, ϕ_N . We note that if $\phi \in \Gamma(\gamma)$, then the geodesic distance between any two phases must be strictly less than γ , that is, $\text{dist}(\phi_i, \phi_j) < \gamma$ for any $i, j \in \{1, \dots, N\}$. The converse is not in general true.

2.3 Synchrony

Synchrony occurs when all N oscillators in the network have the same phase. The network is at synchrony at time t if $\phi(t) \in \Gamma(\epsilon)$ for arbitrarily small $\epsilon \in \mathbb{R}_{\geq 0}$. We can quantify the *error* from synchrony at time t as the length of the smallest arc that contains $\phi(t)$.

2.4 Definitions

The following definitions are used in Theorems 1 to 3:

D.1 Define the *arc length function* $V_{\text{arc-length}} : \mathbb{T}^N \rightarrow [0, 1[$ by

$$V_{\text{arc-length}}(x) = \min_{\substack{s \in [0, 1[, \\ x \in \Gamma(s)}} s,$$

so that $V_{\text{arc-length}}(x)$ is the length of the shortest arc containing x .

D.2 Define the *sensing digraph* as an unweighted digraph \mathcal{G} with vertices $V = \{1, \dots, N\}$. Its edge set is defined as follows: every node has a self-loop. For $i \neq j$, (i, j) is an edge if i can receive a pulse from j . An example of a sensing digraph is shown in Figure 2.2.

D.3 Let d_{\max} be the maximum out-degree of any node in \mathcal{G} (excluding self-loops). Let $|\mathcal{E}|$ be the cardinality of the edge set of \mathcal{G} (excluding self-loops).

D.4 Assuming the sensing digraph \mathcal{G} has a globally reachable node, let b be the smallest number such that the globally reachable node can be reached from **any** node by a path that has most b edges. Note that, if \mathcal{G} has a self-loop on every node, then the globally reachable node can be reached from any node by a path that has **exactly** b edges.

D.5 Let t_1, t_2, \dots be the ordered sequence of times at a pulse is received by any one of the oscillators.

D.6 Define, for $p \in \mathbb{N}$, the *reception digraph* as a weighted digraph \mathcal{G}_p with vertices $\tilde{V} = \{1, \dots, N\}$ and edge set as follows. Every node corresponding to an oscillator that does not receive a pulse at time t_p has a self-loop weighted 1. If at time t_p a pulse is received by oscillator i from oscillator j , then node i has a self-loop weighted $1 - h$, there is an edge from i to j weighted h . We note that each reception digraph can be constructed by taking a sub-graph of the sensing digraph and adding weights on all the edges. Examples of reception digraphs are shown in Figure 2.3.

D.7 Let A_p be the adjacency matrix of \mathcal{G}_p . We note that A_p is *row-stochastic*, that is, it has all non-negative elements and the sum of elements of each row is 1.

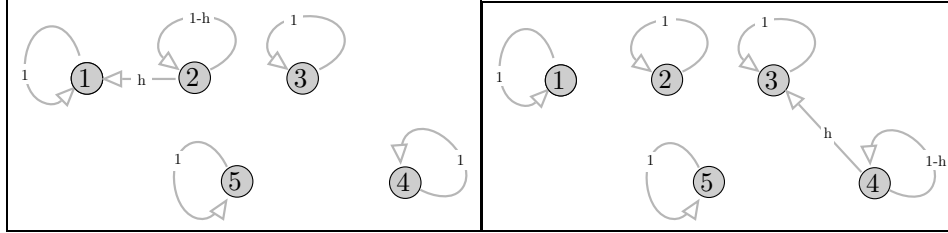


Figure 2.3: Two examples of reception digraphs consistent with the sensing digraph in Figure 2.2, where oscillator 2 receives a pulse from oscillator 1 (on the left) and where oscillator 3 receives a pulse from oscillator 4 (on the right).

3 Estimating Durations Between Pulses

Theorem 1 below describes the timing of the firings and receptions of pulses in the PCO network, based on the properties of the sensing digraph (namely, degree and number of edges) and the pulse strength. The properties described in this section enable us to write the PCO network system equations as an LTV system sampled at the times when a reception occurs, in subsequent sections.

The time at which an oscillator fires is affected by the number of pulses received, and by the phase of the oscillator when the pulses are received. Statement (i) states that if the pulse strength is sufficiently small, then despite the effect of the pulses received, the time between successive firings of a given oscillator is upper- and lower-bounded, and provides an estimate for the upper and lower bounds.

Statement (ii) follows from Statement (i), and states that for a sufficiently large number of receptions, at least one pulse must be received along every (non-self-loop) edge of the sensing digraph.

Statement (iii) provides *upper* bound on the number of pulses received by an oscillator in a sequence of successive receptions of specified length, based on the fact that not all the pulses sent in that duration can repeat on the same edge since some of the pulses must be sent along the other edges as well.

Theorem 1 (Upper and lower bounds on receptions by an oscillator in a sequence of successive receptions). *Consider a PCO network with N oscillators, with arbitrary delays for each edge in the sensing digraph \mathcal{G} , and with pulse strength h . Assume the pulse strength h satisfies*

$$hd_{\max} < 1. \tag{3.1}$$

Then the following statements hold:

- (i) *for any oscillator $i \in \{1, \dots, N\}$ and for all $n \in \mathbb{N}$, the duration $T_{i,n}$ between*

the n th and $(n + 1)$ th firings of i satisfies

$$T_{\min} \leq T_{i,n} \leq T_{\max},$$

where $T_{\min} = \frac{1}{2}$ and $T_{\max} = \frac{1}{2} + \frac{1}{(1-hd_{\max})}$,

(ii) there exists a duration $\delta \leq \delta_{\max} = 1 + \left\lceil 1 + \frac{2}{1-hd_{\max}} \right\rceil (|\mathcal{E}| - 1)$ such that the sensing digraph and the reception digraphs satisfy for all time index $p \in \mathbb{N}$:

$$\mathcal{G}_p \cup \mathcal{G}_{p+1} \cup \dots \cup \mathcal{G}_{p+\delta-1} = \mathcal{G},$$

(iii) the maximum number of pulses received by each oscillator over an interval of duration $v \in \mathbb{N}$ is

$$\mathcal{M}(v) = \left\lfloor \frac{v}{\delta} \right\rfloor (\delta - |\mathcal{E}| + d_{\max}) + \min \{ (v \bmod \delta), (\delta - |\mathcal{E}| + d_{\max}) \}. \quad (3.2)$$

The proof of Statement (i) proceeds as follows. The duration between firings of an oscillator depends on the number of pulses the oscillator receives between its firings. Some pulses move the phase forward, decreasing the duration, and some move the phase backward, increasing the duration to the next firing of the oscillator. The maximum and minimum durations between successive firings of the same oscillator depend on the maximum effect of the pulses. The proofs of Statements (ii) and (iii) follow from Statement (i).

Proof. If an oscillator i receives no pulses from its out-neighbors between its n th and $(n + 1)$ th firing, then from the continuous dynamics equation (2.1), $T_{i,n} = 1$. If oscillator i does receive pulses, then each pulse either increases or decreases the time to the next firing according to the discrete dynamics equation (2.2).

We estimate T_{\min} as follows. Equations (2.1) and (2.2) imply that a pulse received by oscillator i when $\phi_i(t) < \frac{1}{2}$ can only *increase* the time to firing of oscillator i . Hence $T_{i,n} \geq \frac{1}{2}$ for all $n \in \mathbb{N}$, since if no pulses were received $\phi_i(t) < \frac{1}{2}$ then $T_{i,n}$ would be given by $\frac{1}{2}$ plus the positive duration that is taken for the phase to increase from $\frac{1}{2}$ to 1. Therefore $T_{\min} = \frac{1}{2}$.

Next, we estimate T_{\max} as follows. In a duration Δt , a particular out-neighbor of i can fire at most $\lceil \frac{\Delta t}{\tau_{\min}} \rceil = \lceil 2\Delta t \rceil$ times. As a result, in a duration Δt , oscillator i can receive at most $d_i (\lceil 2\Delta t \rceil)$ pulses (since all the τ_{ij} s are constant). From equation (2.2), each pulse results in a phase change of at most $\frac{h}{2}$. Conceivably, each pulse that oscillator i receives could result in a phase change of $\frac{h}{2}$, since the oscillator could receive a pulse when its phase is just less than $\frac{1}{2}$, then move backward by $\frac{h}{2}$, then move forward again to $\frac{1}{2}$ under the continuous dynamics, and then receive another pulse (and so on). Therefore, the total phase change $\Delta\phi_i$ of oscillator i in the duration Δt satisfies the following inequality:

$$\begin{aligned} \Delta\phi_i &\geq \Delta t - \frac{h}{2} (d_i \lceil 2\Delta t \rceil) \geq \Delta t - \frac{h}{2} (d_i 2\Delta t + 1) = (1 - hd_i) \Delta t - \frac{h}{2} d_i \\ &\implies \Delta\phi_i \geq (1 - hd_{\max}) \Delta t - \frac{h}{2} d_{\max}. \end{aligned} \quad (3.3)$$

We see from equations (3.1) and (3.3) that if $\Delta t \geq \frac{1}{(1-hd_{\max})}$, then $\Delta\phi_i \geq \frac{1}{2}$. So the time taken by the oscillator to reach a phase of $\frac{1}{2}$ from 0 is less than or equal to $\frac{1}{(1-hd_{\max})}$, and the time taken by the oscillator to reach a phase of 1 from $\frac{1}{2}$ is less than or equal to $\frac{1}{2}$ since any pulses it receives during this duration will increase the time taken, not decrease it. Therefore, the time taken for the phase to reach 1 from 0 is less than or equal to $T_{\max} := \frac{1}{2} + \frac{1}{(1-hd_{\max})}$. This concludes the proof of statement (i).

To prove statement (ii), we note that if a pulse is received along the edge (i, j) for the n th time at a time t , then the next time a pulse is received along the edge

(i, j) is $t + T_{j,n}$ since the delay τ_{ij} is constant. Therefore, the duration between successive receptions of pulses along the the edge (i, j) is $T_{j,n}$ for some $n \in \mathbb{N}$. The total number of receptions during the interval $]t, t + T_{j,n}]$ is less than or equal to $1 + \left\lceil \frac{T_{j,n}}{T_{\min}} \right\rceil (|\mathcal{E}| - 1)$, considering the receptions on all the other $(|\mathcal{E}| - 1)$ edges as well. Since $T_{j,n} \leq T_{\max}$, this implies that there exists a number δ which is less than $\delta_{\max} := 1 + \left\lceil \frac{T_{\max}}{T_{\min}} \right\rceil (|\mathcal{E}| - 1) = 1 + \left\lceil 1 + \frac{2}{1 - hd_{\max}} \right\rceil (|\mathcal{E}| - 1)$, such that every sequence of δ successive receptions must contain at least one reception along every edge of \mathcal{G} , and hence the union of the digraphs $\mathcal{G}_p \cup \mathcal{G}_{p+1} \cup \dots \cup \mathcal{G}_{p+\delta-1}$ is \mathcal{G} , for all $p \in \mathbb{N}$. This concludes the proof of statement (ii).

Finally, to prove statement (iii) we estimate the number of pulses received by a particular oscillator i during v successive receptions. We note that in a sequence of δ successive firings, at least one reception must occur along each of the $|\mathcal{E}| - d_i$ edges that are not from node i . This implies that the maximum number of pulses that an oscillator may receive in a sequence of δ successive receptions is $\delta - |\mathcal{E}| + d_{\max}$. The maximum number of pulses received by an oscillator in a sequence of v successive receptions, $\mathcal{M}(v)$ can be estimated by breaking the sequence into parts of length δ . Therefore, we know $\mathcal{M}(v) = \left\lfloor \frac{v}{\delta} \right\rfloor (\delta - |\mathcal{E}| + d_{\max}) + \min \{v \bmod \delta, (\delta - |\mathcal{E}| + d_{\max})\}$. This concludes the proof of the theorem. \square

4 Synchronization with No Delays

In this section we show that, if all the delays in the pulse-transmission are zero, and the pulse strength is sufficiently small, and the sensing digraph has a globally reachable node, then the PCO network synchronizes exactly for all initial conditions contained within an arc of length $\frac{1}{2}$. Furthermore, the error from synchrony (quantified by the arc length function $V_{\text{arc-length}}$) decreases exponentially with the time index.

Theorem 2 (Exponential synchronization). *Consider a PCO network with N oscillators, with delays $\tau_{ij} = 0$ for each edge (i, j) in the sensing digraph \mathcal{G} , and with pulse strength h . Assume that*

(A1): *the sensing digraph \mathcal{G} has a globally reachable node, and*

(A2): *the pulse strength h satisfies equation (3.1): $hd_{\max} < 1$.*

Then, the PCO network synchronizes exponentially for all initial conditions $\phi(0)$ contained within an arc of length $\frac{1}{2}$. More precisely, if $\delta \leq \delta_{\max}$ is the smallest number in \mathbb{N} such that:

$$\mathcal{G}_p \cup \mathcal{G}_{p+1} \cup \dots \cup \mathcal{G}_{p+\delta-1} = \mathcal{G},$$

for any $p \in \mathbb{N}$, then the following equation is satisfied:

$$V_{\text{arc-length}}(\phi(t_{m\Delta})) \leq a V_{\text{arc-length}}(\phi(t_{m\Delta-\Delta})), \quad \text{for all } m \in \mathbb{N}, \text{ if } \phi(0) \in \Gamma\left(\frac{1}{2}\right), \quad (4.1)$$

where $\Delta = b\delta$ and $a = (1 - \min\{h, 1 - h\})^b (1 - h)^{b(\delta - |\mathcal{E}| + d_{\max} - 1)} \in]0, 1[$.

The proof of Theorem 2 proceeds as follows. The vector of phases $\phi(t)$ is transformed to a coordinate system that rotates at the same rate as the continuous dynamics of the oscillators, so that the transformed phase vector $\tilde{\phi}(t)$ remains constant

between receptions and only the discrete dynamics remain. Then, the discrete dynamics is rewritten as a first-order LTV system, using the adjacency matrices of the reception digraphs. A theorem on distributed time-varying consensus from [2] is shown to be applicable to the discrete dynamics, and conditions for exponential convergence are derived. Additionally, the rate of convergence is quantified using Theorem 1.

Proof. **Coordinate Transformation**

Define a rotating coordinate system with its origin $c(t) \in [0, 1[$ such that:

- The origin has the continuous dynamics as the oscillators, or, $\dot{c}(t) = 1$.
- When the phase $c(t)$ reaches 1, it is reset to 0.
- The origin lies within an arc of length $\frac{1}{2}$ that also contains $\phi(0)$ at $t = 0$, such that

$$0_N \leq \phi(0) - c(0) \mathbf{1}_N < \frac{1}{2} \mathbf{1}_N. \quad (4.2)$$

Such an origin can be found if $\phi(0) \in \Gamma(\frac{1}{2})$.

The transformed phase vector $\tilde{\phi}(t)$ is given by:

$$\tilde{\phi}(t) = \text{dist}_{\text{cc}}(c(t), \phi(t)), \quad (4.3)$$

as shown in Figure 4.1. Clearly, the derivative of $\tilde{\phi}(t)$ under the continuous dynamics in equation (2.1) is zero so the transformed phase vector remains constant at all times except during receptions. The origin of the fixed coordinate system is expressed in the rotating coordinate system as $\tilde{\phi}_0(t)$ and moves clockwise such that:

$$\dot{\tilde{\phi}}_0(t) = -1. \quad (4.4)$$

When a pulse is received, the receiving oscillators move toward the origin of the fixed coordinate system, according to equation (2.2). Considering equation (4.2), the discrete dynamics of the transformed phase vector is given by rewriting equation (2.2) as follows:

$$\tilde{\phi}_i(t_{p+1}) = \begin{cases} \tilde{\phi}_i(t_p) - h \left(\tilde{\phi}_i(t_p) - \tilde{\phi}_0(t_p) \right), & \tilde{\phi}_i(t_p) - \tilde{\phi}_0(t_p) \in [0, \frac{1}{2}[\\ \tilde{\phi}_i(t_p) + h - h \left(\tilde{\phi}_i(t_p) - \tilde{\phi}_0(t_p) \right), & \tilde{\phi}_i(t_p) - \tilde{\phi}_0(t_p) \in [\frac{1}{2}, 1], \end{cases}$$

for all i such that oscillator i receives a pulse at time t_p , and

$$\tilde{\phi}_i(t_{p+1}) = \tilde{\phi}_i(t_p) \tag{4.5}$$

for all i such that oscillator i does not receive a pulse at time t_p .

We note that since $\tilde{\phi}(t)$ remains constant between t_p^+ and t_{p+1} , $\tilde{\phi}_i(t_p^+)$ is replaced with $\tilde{\phi}_i(t_{p+1})$ in equation (4.5).

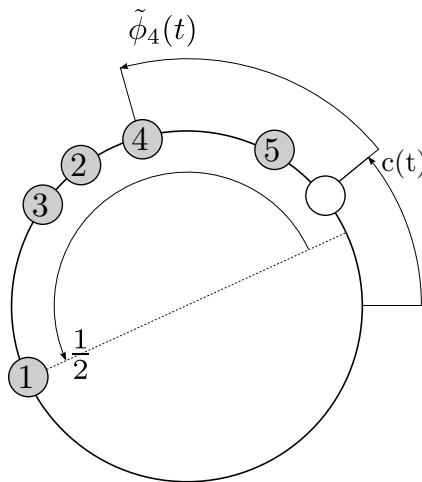


Figure 4.1: The coordinate transformation from $\phi(t)$ to $\tilde{\phi}(t)$ in the rotating coordinate frame. The origin of rotating coordinate frame is at a counterclockwise distance of $c(t)$ from the origin of the fixed coordinate frame.

Rewriting the Discrete Dynamics as an LTV System

Suppose the pulse received at time t_p was sent by oscillator j . Since $\tau_{ij} = 0$, the oscillator j must have fired at the same instant t_p , and hence its phase coincides with the origin of the fixed coordinate system, or $\tilde{\phi}_0(t_p) = \tilde{\phi}_j(t_p)$, which can be substituted in equation (4.5) to obtain the following:

$$\tilde{\phi}_i(t_{p+1}) = \begin{cases} (1-h)\tilde{\phi}_i(t_p) + h\tilde{\phi}_j(t_p), & \tilde{\phi}_i(t_p) - \tilde{\phi}_j(t_p) \in [0, \frac{1}{2}[\\ (1-h)\tilde{\phi}_i(t_p) + h + h\tilde{\phi}_j(t_p), & \tilde{\phi}_i(t_p) - \tilde{\phi}_j(t_p) \in [\frac{1}{2}, 1]. \end{cases}$$

for all i such that oscillator i receives a pulse at time t_p , and

$$\tilde{\phi}_i(t_{p+1}) = \tilde{\phi}_i(t_p) \tag{4.6}$$

for all i such that oscillator i does not receive a pulse at time t_p .

We observe from equation (4.6) that if the following condition:

$$0_N \leq \phi(t_p) \leq \frac{1}{2}\mathbb{1}_N \tag{4.7}$$

is satisfied at time t_p , then if i receives a pulse at t_p ,

$$\tilde{\phi}_i(t_{p+1}) = (1-h)\tilde{\phi}_i(t_p) + h\tilde{\phi}_j(t_p).$$

Since $\tilde{\phi}_i(t_{p+1})$ is a convex combination of the elements of $\tilde{\phi}_i(t_p)$, the condition (4.7) is satisfied at t_{p+1} as well. And since the condition (4.7) is satisfied at $t = 0$, the condition (4.7) is satisfied for all $t > 0$. As a result, the piece-wise form of (4.6) can be discarded and the discrete dynamics can be rewritten using the definition of A_p , as given below:

$$\tilde{\phi}(t_{p+1}) = A_p \tilde{\phi}(t_p). \tag{4.8}$$

Global Reachability Over Time in the Reception Digraphs

Equation (4.8) is a time-varying distributed averaging algorithm that satisfies the following conditions:

- The adjacency matrices of the reception digraphs are row-stochastic.
- The reception digraphs \mathcal{G}_p have self-loops on every node.
- Every element of the adjacency matrix of the reception digraph belongs to the set $\{0, h, 1 - h, 1\}$.
- There exists a number $\delta \leq \delta_{\max}$ such that the union of any δ successive reception digraphs has a globally reachable node.

We use a method based on [2], adapted to the PCO network system, to show that above four conditions are sufficient for the vector $\tilde{\phi}(t_p)$ to synchronize, with the length of the smallest arc containing the phase vector decreasing exponentially to zero. First we show that the globally reachable node of \mathcal{G} , which we will denote as r , is reachable from any node over the sequence of $\Delta := b\delta$ successive reception digraphs, in the following sense: for every $k \in \{1, \dots, N\}$, there exists a sequence of nodes $\{k, i_1, i_2, \dots, i_{\Delta-1}, r\}$ such that (k, i_1) is an edge of \mathcal{G}_p , (i_w, i_{w+1}) is an edge in \mathcal{G}_{p+w} , $w = 1, \dots, \Delta - 1$ and $\{i_{\Delta-1}, r\}$ is an edge in $\mathcal{G}_{p+\Delta}$.

Suppose (i, j) is an edge in \mathcal{G} . From Theorem 1 (ii), the edge (i, j) must appear in at least one digraph in the sequence $\mathcal{G}_p, \mathcal{G}_{p+1}, \dots, \mathcal{G}_{p+\delta-1}$. Suppose the edge exists in \mathcal{G}_{p+w} , where $0 \leq w \leq \delta$. Then, node j is reachable from i over the duration $\{p, p + \delta - 1\}$, since the following ordered sequence of $\delta + 1$ nodes exists:

$$\left\{ \begin{array}{cc} i, \dots, i & j, \dots, j \\ w \text{ times} & \delta - w + 1 \text{ times} \end{array} \right\},$$

such that:

- the edge (i, i) exists in the digraphs $\mathcal{G}_p, \mathcal{G}_{p+1}, \dots, \mathcal{G}_{p+w-1}$ (since there are self-loops on every node of the digraphs),
- the edge (i, j) exists in the digraph \mathcal{G}_{p+w} by our assumption, and
- and the edges (j, j) exist in the digraphs $\mathcal{G}_{p+w+1}, \mathcal{G}_{p+w+2}, \dots, \mathcal{G}_{p+\delta-1}$ (since there are self-loops on every node of the digraphs).

So if (i, j) is an edge in \mathcal{G} , then node i is reachable from j in the sequence of reception digraphs, over every duration of length δ or greater. We observe from Theorem 1(iii) that at most $\delta - |\mathcal{E}| + d_{\max}$ edges in the above sequence are weighted less than 1 (these edges are associated with pulses received by i or j), and that at most one edge in the above sequence is weighted h (the edge from i to j if they are distinct).

Since there is a path of b edges from every node k to r in \mathcal{G} from the definition **D.4**, we can construct a sequence of $b\delta + 1$ nodes starting with k and ending with r , over every sequence of $b\delta$ successive reception digraphs, by concatenating a sequence like the one described above for each edge of the path (and discarding the repeated node at the point of concatenation). Hence the node r is reachable from every node k over a every sequence of $b\delta = \Delta$ successive reception digraphs. We note that at most $b(\delta - |\mathcal{E}| + d_{\max})$ edges in the above sequence are weighted less than 1, and that at most b edges in the sequence of edges to reach r are weighted h .

We use the property of global reachability of r in the reception digraphs to analyze the linear time-varying system of the PCO network.

Exponential Convergence of the Arc Length

Let \mathcal{A} denote the product $A_{m_{\Delta+\Delta-1}}A_{m_{\Delta+\Delta-2}}\dots A_{m_{\Delta}}$. Consider the equation obtained by applying equation (4.5) recursively Δ times, to calculate $\tilde{\phi}(t_{m_{\Delta+\Delta}})$ from

$\tilde{\phi}(t_{m\Delta})$:

$$\begin{aligned}\tilde{\phi}(t_{m\Delta+\Delta}) &= A_{m\Delta+\Delta-1}A_{m\Delta+\Delta-2}\dots A_{m\Delta}\tilde{\phi}(t_{m\Delta}) \\ &= \mathcal{A}\tilde{\phi}(t_{m\Delta}).\end{aligned}\tag{4.9}$$

Let $a_{ij}(p)$ denote the (i, j) element of A_p . For a node k , consider a sequence of nodes $\{k, i_1, \dots, i_{\Delta-1}, r\}$ such that (k, i_1) is an edge in $\mathcal{G}_{m\Delta}$, (i_w, i_{w+1}) is an edge in $\mathcal{G}_{m\Delta+w}$ for $w = \{1, \dots, m\Delta + \Delta - 2\}$, and $(i_{\Delta-1}, r)$ is an edge in $\mathcal{G}_{m\Delta+\Delta-1}$. This means that $a_{k,i_1}(m\Delta) \geq \min\{h, 1-h\}$, $a_{i_w,i_{w+1}}(m\Delta+w) \geq \min\{h, 1-h\}$ for $w = \{1, \dots, m\Delta + \Delta - 2\}$, and $a_{i_{\Delta-1},r}(m\Delta + \Delta - 1) \geq \min\{h, 1-h\}$. Furthermore, at most b of these elements are equal to h .

We note that since \mathcal{A} is a product of row-stochastic matrices, \mathcal{A} is row-stochastic [2]. The method in [2] uses the observation that the product:

$$a_{k,i_1}(m\Delta) a_{i_1,i_2}(m\Delta+1) \dots a_{i_{\Delta-2},i_{\Delta-1}}(m\Delta+\Delta-2) a_{i_{\Delta-1},r}(m\Delta+\Delta-1)$$

is one term in the expression for \mathcal{A}_{kr} , and that all the other terms are non-negative.

Hence:

$$\mathcal{A}_{kr} \geq \eta := \min\{h, 1-h\}^b (1-h)^{b(\delta-|\mathcal{E}|+d_{\max}-1)} \quad \text{for all } k \in \{1, \dots, N\}.\tag{4.10}$$

We further observe, by expanding the matrix-multiplication in equation (4.9),

that:

$$\begin{aligned}
\tilde{\phi}_k(t_{m\Delta+\Delta}) &= \mathcal{A}_{kr}\tilde{\phi}_r(t_{m\Delta}) + \sum_{i \neq r, i=1}^N \mathcal{A}_{ki}\tilde{\phi}_i(t_{m\Delta}) \\
&\leq \tilde{\mathcal{A}}_{kr}\tilde{\phi}_r(t_{m\Delta}) + (1 - \mathcal{A}_{kr}) \max\left(\tilde{\phi}(t_{m\Delta})\right) \\
&\text{(since } \mathcal{A} \text{ is row-stochastic)} \\
&\leq \eta\tilde{\phi}_r(t_{m\Delta}) + (1 - \eta) \max\left(\tilde{\phi}(t_{m\Delta})\right) \text{ for all } k \\
&\text{(from (4.10)).} \\
\implies \max\left(\tilde{\phi}(t_{m\Delta+\Delta})\right) &\leq \eta\tilde{\phi}_r(t_{m\Delta}) + (1 - \eta) \max\left(\tilde{\phi}(t_{m\Delta})\right) \tag{4.11}
\end{aligned}$$

By a similar argument, we can also show that:

$$\min\left(\tilde{\phi}(t_{m\Delta+\Delta})\right) \geq \eta\tilde{\phi}_r(t_{m\Delta}) + (1 - \eta) \min\left(\tilde{\phi}(t_{m\Delta})\right) \tag{4.12}$$

Lastly, we note that since $\phi(t) \in \Gamma\left(\frac{1}{2}\right)$, the arc length $V_{\text{arc-length}}(\phi(t))$ is simply given by:

$$\begin{aligned}
V_{\text{arc-length}}(\phi(t)) &= \max\left(\tilde{\phi}(t)\right) - \min\left(\tilde{\phi}(t)\right) \\
\implies V_{\text{arc-length}}(\phi(t_{m\Delta+\Delta})) &= \max\left(\tilde{\phi}(t_{m\Delta+\Delta})\right) - \min\left(\tilde{\phi}(t_{m\Delta+\Delta})\right) \\
&\leq (1 - \eta) \left(\max\left(\tilde{\phi}(t_{m\Delta})\right) - \min\left(\tilde{\phi}(t_{m\Delta})\right) \right) \\
&\text{(from (4.11) and (4.12))} \\
&\leq a V_{\text{arc-length}}(\phi(t_{m\Delta})),
\end{aligned}$$

where $a = 1 - \eta$. □

5 Synchronization with Delays

Theorem 3 below states that if all the delays are sufficiently small, and the pulse strength is sufficiently small, and the sensing digraph has a globally reachable node, then the PCO network synchronizes approximately, for all initial conditions contained within an arc of a specified length.

In other words, the error from synchrony, quantified by the arc length function, converges exponentially with the time index p (sampled at multiples of a number $\tilde{\Delta}$) to a final value that is proportional to the maximum delay τ_{\max} . Between samples, the arc length function may deviate from the exponential curve by an additive factor.

Theorem 3 (Exponential synchronization with delays). *Consider a PCO network with N oscillators, with delays τ_{ij} for each edge (i, j) in the sensing digraph \mathcal{G} , and with pulse strength h . Suppose $\delta \leq \delta_{\max}$ is the smallest number in \mathbb{N} such that:*

$$\mathcal{G}_p \cup \mathcal{G}_{p+1} \cup \dots \cup \mathcal{G}_{p+\delta-1} = \mathcal{G},$$

for any $p \in \mathbb{N}$. Assume that:

(A1) the sensing digraph \mathcal{G} has a globally reachable node,

(A2) the pulse strength h satisfies equation (3.1): $h\delta_{\max} < 1$, and

(A3) the maximum delay τ_{\max} and the pulse strength h satisfy the following inequality:

$$\left(\frac{1 - (1 - h)^{\mathcal{M}(\tilde{\Delta})}}{\min\{h, 1 - h\}^b (1 - h)^{b(3(\delta - |\mathcal{E}| + d_{\max}) - 1)}} + \frac{1}{(1 - h)^{\mathcal{M}(\tilde{\Delta})}} \right) \tau_{\max} < \frac{1}{2}, \quad (5.1)$$

where $\tilde{\Delta} = b(\delta + |\mathcal{E}|)$.

Then, there exists a function $V : \mathbb{N} \rightarrow [0, 1[$ such that $V(0) = V_{\text{arc-length}}(\phi(0))$

and $V_{\text{arc-length}}(\phi(t_{m\tilde{\Delta}})) \leq V(m\tilde{\Delta})$ for all $m \in \mathbb{N}$, and:

$$V(m\tilde{\Delta} + \tilde{\Delta}) - V_{\text{final}} \leq \tilde{a} \left(V(m\tilde{\Delta}) - V_{\text{final}} \right), \quad \text{for all } m \in \mathbb{N},$$

$$\text{if } \phi(0) \in \Gamma \left(\frac{1}{2} - l_0 - \tau_{\text{max}} \right),$$

where:

- $\tilde{\Delta} = b(\delta + |\mathcal{E}|)$,
- $\tilde{a} = \left(1 - \min\{h, 1-h\}^b (1-h)^{b(3(\delta-|\mathcal{E}|+d_{\text{max}})-1)} \right) \in]0, 1[$,
- $V_{\text{final}} = \frac{1}{1-\tilde{a}} \left(1 - (1-h)^{\mathcal{M}(\tilde{\Delta})} \right) \tau_{\text{max}}$,
- $l_0 = \left(\frac{1}{(1-h)^{\mathcal{M}(\tilde{\Delta})}} - 1 \right) \tau_{\text{max}}$.

The proof of Theorem 3 is by induction. For a given start time, assuming the phases are contained in a sufficiently small arc, the proof proceeds along the lines of the proof of Theorem 2. The vector of phases of the oscillators, $\phi(t)$ is transformed to a coordinate system that rotates at the same rate as the continuous dynamics of the oscillators, so that the transformed phase vector $\tilde{\phi}(t)$ remains constant between receptions (i.e., only the discrete dynamics remain).

Then, the discrete dynamics is rewritten as a non-homogeneous higher-order LTV system. A modified reception digraph is constructed by adding additional nodes that store previous values of the phases of the oscillators. The discrete dynamics is then converted to a first-order system using the adjacency matrices of the modified reception digraphs. The method used to prove the theorem on distributed time-varying consensus from [2] is used to derive conditions for exponential convergence. Additionally, we estimate the rate of convergence by using Theorem 1.

Finally, we prove that if the arc length was sufficiently small at the start time for the linear time-varying system equations to be valid, then the arc length is also sufficiently small after $\tilde{\Delta}$ samples after the start time, and hence (by induction)

the condition on the *initial* phase is sufficient for the linear time-varying system equations to be valid for all $t \in \mathbb{R}_{\geq 0}$.

Proof. **Coordinate Transformation**

Assume that at some start time $p = y$, the following condition is satisfied:

$$\phi(t_y) \in \Gamma \left(\frac{1}{2} - l_0 - \tau_{\max} \right). \quad (5.2)$$

Define a rotating coordinate system with its origin $c(t) \in [0, 1[$ such that:

- The origin has the same continuous dynamics as the oscillators, or, $\dot{c}(t) = 1$.
- When the phase $c(t)$ reaches 1, it is reset to 0.
- The origin lies within an arc of length $\frac{1}{2} - l_0$ that also contains $\phi(t_y)$ at $t = t_y$, such that

$$l_0 \mathbf{1}_N \leq \phi(t_y) - c(t_y) \mathbf{1}_N < \left(\frac{1}{2} - \tau_{\max} \right) \mathbf{1}_N. \quad (5.3)$$

Such an origin can be found if since condition (5.2) is satisfied at t_y .

As in the proof of Theorem 2, the transformed $\tilde{\phi}(t)$ is given by equation (4.3). The derivative of $\tilde{\phi}(t)$ under the continuous dynamics in equation (2.1) is zero so the transformed phase vector remains constant at all times except during receptions. The origin of the fixed coordinate system is expressed in the rotating coordinate system as $\tilde{\phi}_0(t)$ and moves clockwise according to equation (4.4). The discrete dynamics of the transformed phases are given by equation (4.5).

Rewriting the Discrete Dynamics as an LTV System with Disturbances

Suppose oscillator i receives a pulse from oscillator j at time t_p . As in the proof of Theorem 2, we solve for $\tilde{\phi}_0(t_p)$ in terms of the phase of oscillator j and substitute

in equation (4.5). Oscillator j fired at time $t_p - \tau_{ij}$, so $\tilde{\phi}_j = \tilde{\phi}_0$ at time $t_p - \tau_{ij}$. We solve for $\tilde{\phi}_0(t_p)$ as follows:

$$\begin{aligned}\tilde{\phi}_j(t_p - \tau_{ij}) &= \tilde{\phi}_0(t_p - \tau_{ij}) \\ &= \tilde{\phi}_0(t_p) + \tau_{ij} \quad (\text{from equation (4.4)}) \\ \implies \tilde{\phi}_0(t_p) &= \tilde{\phi}_j(t_p - \tau_{ij}).\end{aligned}\tag{5.4}$$

Suppose q receptions of pulses (by any oscillator) occurred in the duration $]t_p - \tau_{ij}, t_p[$. Then, $\phi_j(t_p - \tau_{ij}) = \phi_j(t_{p-q})$, and $\tilde{\phi}_0(t_p)$ is given by the following equation:

$$\tilde{\phi}_0(t_p) = \tilde{\phi}_j(t_{p-q}) - \tau_{ij}.\tag{5.5}$$

The discrete dynamics is rewritten by substituting equation (5.5) in equation (4.5) to obtain the following:

$$\tilde{\phi}_i(t_{p+1}) = \begin{cases} (1-h)\tilde{\phi}_i(t_p) + \tilde{\phi}_j(t_{p-q}) - h\tau_{ij}, & \tilde{\phi}_i(t_{p-q}) - \tilde{\phi}_j(t_p) + \tau_{ij} \in [0, \frac{1}{2}[\\ (1-h)\tilde{\phi}_i(t_p) + h + \tilde{\phi}_j(t_{p-q}) - h\tau_{ij}, & \tilde{\phi}_i(t_{p-q}) - \tilde{\phi}_j(t_p) + \tau_{ij} \in [\frac{1}{2}, 1]. \end{cases}$$

for all i such that oscillator i receives a pulse at time t_p , and

$$\tilde{\phi}_i(t_{p+1}) = \tilde{\phi}_i(t_p)\tag{5.6}$$

for all i such that oscillator i does not receive a pulse at time t_p .

Equation (5.6) may be of order greater than one. From Theorem 1 (i), the maximum number of times a given oscillator could have fired in the duration $]t_p - \tau_{ij}, t_p[$ is given by

$$\lceil \frac{\tau_{\max}}{T_{\min}} \rceil = 1$$

since $\tau_{\max} < \frac{1}{2}$. Therefore q must be less than or equal to the number of edges in the

sensing digraph, $|\mathcal{E}|$. We can express equation (5.6) as a first order system with the modified state vector $x(t) \in \mathbb{R}^{N|\mathcal{E}|+N}$ where $x(t_p) = [\tilde{\phi}(t_p)^T \dots \tilde{\phi}(t_{p-|\mathcal{E}|})^T]^T$. The discrete dynamics is then described by the following equations (note that we use x_i^p to denote $x_i(t_p)$, for brevity):

$$x_i^{p+1} = \begin{cases} (1-h)x_i^p + hx_{j+q|\mathcal{E}|}^p - h\tau_{ij}, & x_i^p - x_{j+q|\mathcal{E}|}^p + \tau_{ij} \in [0, \frac{1}{2}[\\ (1-h)x_i^p + h + hx_{j+q|\mathcal{E}|}^p - h\tau_{ij}, & x_i^p - x_{j+q|\mathcal{E}|}^p + \tau_{ij} \in [\frac{1}{2}, 1]. \end{cases}$$

for all $i \leq N$ such that oscillator i receives a pulse at time t_p , and

$$x_i^{p+1} = x_i^p$$

for all $i \leq N$ such that oscillator i does not receive a pulse at time t_p

$$x_i^{p+1} = x_{i-|\mathcal{E}|}^p \tag{5.7}$$

for all $i \in \{N+1, \dots, N|\mathcal{E}|+N\}$.

We can discard the piece-wise structure of system equations (5.7) as we did in the proof of Theorem 2, if we ensure that the phase vector remains within a sufficiently small arc, as follows. We know that if the following condition:

$$0_N \leq x^p \leq \left(\frac{1}{2} - \tau_{\max}\right) \mathbf{1}_N \tag{5.8}$$

is satisfied at time t_p , then the system equation is

$$x_i^{p+1} \geq (1-h)x_i^p - h\tau_{\max}. \tag{5.9}$$

if i receives a pulse at time t_p , and x_i remains unchanged if i does not receive a pulse at t_p . However, depending on τ_{\max} , the arc length may have increased at t_p ,

and condition (5.8) may be violated at t_{p+1} . Therefore, in order to apply the above equation recursively v times, we must further restrict the arc of phases at t_y , such that even after a duration v , the increase in the the arc length does not cause condition (5.8) to be violated at t_{y+v} .

We know from Theorem 1 (iii) that in a duration of length v , an oscillator can receive at most $\mathcal{M}(v)$ pulses. This implies that if the following condition is satisfied at time t_y :

$$\left(\frac{1}{(1-h)^{\mathcal{M}(v)}} - 1 \right) \tau_{\max} \mathbf{1}_N \leq x^p \leq \left(\frac{1}{2} - \tau_{\max} \right) \mathbf{1}_N, \quad (5.10)$$

then equation (5.9) can be applied recursively $\mathcal{M}(v)$ times to yield the following inequality:

$$\begin{aligned} x^{y+v} &\geq (1-h)^{\mathcal{M}(v)} x^y - \left(1 - (1-h)^{\mathcal{M}(v)} \right) \tau_{\max} \mathbf{1}_N \\ &\geq 0, \end{aligned} \quad (5.11)$$

which means that the condition (5.8) is satisfied at t_{y+1}, \dots, t_{y+v} as well. Then the piece-wise form of (5.7) can be discarded and the discrete dynamics can be rewritten for $p \in \{y, \dots, y+v\}$ as an affine function in x . In order to do this, we now introduce the *modified* reception digraph (MRD), whose the adjacency matrix is \tilde{A}_p .

At time t_p , we define the modified reception digraph $\tilde{\mathcal{G}}_p$. The $N|\mathcal{E}| + N$ vertices of $\tilde{\mathcal{G}}_p$ are defined as follows: for every node k in \mathcal{G}_p , define $|\mathcal{E}| + 1$ nodes in $\tilde{\mathcal{G}}_p$: $k, k^{1-}, k^{2-}, \dots, k^{|\mathcal{E}|-}$. The node k will be sometimes referred to as k^{0-} . The edge set is given as follows:

- There is an edge weighted 1 from every node k^{w-} to $k^{(w+1)-}$, $w = 0, 1, \dots, |\mathcal{E}| - 1$.
- If node i has a self-loop in \mathcal{G}_p , then node i has a self-loop with the same weight in $\tilde{\mathcal{G}}_p$.

- If there is an edge (i, j) for some $i \neq j$ in \mathcal{G}_p , then there is an edge (i, j^{q-}) in $\tilde{\mathcal{G}}_p$, where q is the number of receptions that occurred in the duration $]t_p - \tau_{ij}, t_p[$.

An example of an MRD is shown in Figure 5.1. We note that if there is a path from some node j to a node k in \mathcal{G}_p , then there must be a path from node j to a node k in $\tilde{\mathcal{G}}_p$. Therefore, since we know there is a globally reachable node in $\mathcal{G}_p \cup \mathcal{G}_{p+1} \cup \dots \cup \mathcal{G}_{p+\delta-1}$ from Theorem 1(ii), there must be a globally reachable node in $\tilde{\mathcal{G}}_p \cup \tilde{\mathcal{G}}_{p+1} \cup \dots \cup \tilde{\mathcal{G}}_{p+\delta-1}$ as well.

The added nodes store the old states, such that node k^{w-} has the state $\tilde{\phi}_k(t_{p-w})$, where $w \in \{0, 1, \dots, |\mathcal{E}|\}$. Let the adjacency matrix of $\tilde{\mathcal{G}}_p$ be \tilde{A}_p . Then equation (5.7) can be rewritten as follows if condition (5.10) is satisfied:

$$x^{p+1} = \tilde{A}_p x^p + \tilde{B}_p h \tau_p \quad \text{for } p \in \{1, \dots, m\}, \quad (5.12)$$

where $\tilde{B}_p \in \mathbb{R}^{N|\mathcal{E}|+N}$ has -1 in the i th position and zeros elsewhere, and τ_p is the sum of τ_{ij} over all j such that oscillator i receives a pulse from oscillator j at t_p .

Global Reachability Over Time in the Modified Reception Digraphs

Equation (5.12) is a time-varying distributed averaging algorithm that satisfies the following conditions:

- The adjacency matrices of the MRD are row-stochastic.
- Every element of the adjacency matrix of the MRD belongs to the set $\{0, h, 1 - h, 1\}$.
- There exists a number $\delta \leq \delta_{\max}$ such that the union of any δ successive MRDs has a globally reachable node.

We use a method similar to that in the proof of Theorem 2 to show that above three conditions are sufficient for the arc length $V_{\text{arc-length}}(\tilde{\phi})$ to converge exponentially. First we show that the globally reachable node r of \mathcal{G} , is reachable from

any node of the MRD over the sequence of $\tilde{\Delta} := b(\delta + |\mathcal{E}|)$ successive MRDs, in the following sense: for every $k \in \{1, \dots, N\}$, there exists a sequence of nodes $\{k, i_1, i_2, \dots, i_{\Delta-1}, r\}$ such that (k, i_1) is an edge of $\tilde{\mathcal{G}}_p$, (i_w, i_{w+1}) is an edge in $\tilde{\mathcal{G}}_{p+w}$, $w = 1, \dots, \Delta - 1$ and $\{i_{\Delta-1}, r\}$ is an edge in $\tilde{\mathcal{G}}_{p+\Delta}$.

Suppose (i, j) is an edge in \mathcal{G} . From Theorem 1 (ii), the edge (i, j) must appear in at least one digraph in the sequence $\mathcal{G}_p, \mathcal{G}_{p+1}, \dots, \mathcal{G}_{p+\delta-1}$. Suppose the edge exists in \mathcal{G}_{p+w} , where $0 \leq w \leq \delta$. From the definition of MRD, (i, j^{q-}) must be an edge in $\tilde{\mathcal{G}}_{p+w}$ for some $q \leq |\mathcal{E}|$. Then, node j is reachable from i over the duration $\{p, p + |\mathcal{E}| + \delta - 1\}$, since the following sequence of $\delta + |\mathcal{E}| + 1$ nodes exists:

$$\left\{ \begin{array}{ccc} i, \dots, i, & j^{q-}, j^{(q-1)-}, \dots, j^{1-}, & j, \dots, j \\ \begin{array}{c} w \text{ times} \end{array} & & \begin{array}{c} \delta - w + 1 + |\mathcal{E}| - q \text{ times} \end{array} \end{array} \right\},$$

such that:

- the edges (i, i) exists in the digraphs $\tilde{\mathcal{G}}_p, \tilde{\mathcal{G}}_{p+1}, \dots, \tilde{\mathcal{G}}_{p+w-1}$ (since there are self-loops on every node of the MRD that is also a node in the reception digraphs),
- the edge (i, j^{q-}) exists in $\tilde{\mathcal{G}}_{p+w}$ by our assumption,
- the edges $(j^{q-}, j^{(q-1)-}), (j^{(q-1)-}, j^{(q-2)-}), \dots, (j^{1-}, j)$ exist in $\tilde{\mathcal{G}}_{p+w+1}, \dots, \tilde{\mathcal{G}}_{p+w+q+1}$ respectively (since these edges exist in every MRD), and
- the edges (j, j) exist in the digraphs $\tilde{\mathcal{G}}_{p+w+q+2}, \dots, \tilde{\mathcal{G}}_{p+\delta+|\mathcal{E}|}$, (since there are self-loops on every node of the MRD that is also a node in the reception digraphs).

Therefore if (i, j) is an edge in \mathcal{G} , then node i is reachable from j over every duration of length $\delta + |\mathcal{E}|$ or greater, in the sequence of MRD. We observe from Theorem 1(iii) that at most $\left(1 + \frac{|\mathcal{E}|}{\delta}\right) (\delta - |\mathcal{E}| + d_{\max})$ edges in the above sequence are weighted less than 1 (these edges are associated with pulses received by i or j), and that at most one edge in the above sequence is weighted h (the edge from i to j if they are distinct).

Since there is a path of b edges from every node k to r in \mathcal{G} from the definition **D.4**, we can construct a sequence of $b(\delta + |\mathcal{E}|) + 1$ nodes starting with k and ending with r , over every sequence of $b(\delta + |\mathcal{E}|)$ successive MRDs, by concatenating a sequence like the one described above for each edge of the path (and discarding the repeated node at the point of concatenation). Hence the node r is reachable from every node k over a every sequence of $b(\delta + |\mathcal{E}|) = \Delta$ successive MRDs. We note that at most $b\left(1 + \frac{|\mathcal{E}|}{\delta}\right)(\delta - |\mathcal{E}| + d_{\max})$ edges in the above sequence are weighted less than 1, and that at most b edges in the sequence of edges to reach r are weighted h .

We use the property of global reachability of r in the MRD to analyze the linear time-varying system of the PCO network.

Exponential Convergence of the Arc Length in the Presence of Delays

Assume $y = m\tilde{\Delta}$ and $v = \tilde{\Delta}$. Then, equation (5.10) implies that the system dynamics is given by applying equation (5.12) $\tilde{\Delta}$ times recursively, since $l_0\mathbf{1}_N \leq x^y \leq \left(\frac{1}{2} - \tau_{\max}\right)\mathbf{1}_N$ from our choice of coordinate system, where:

$$l_0 = \left(\frac{1}{(1-h)^{\mathcal{M}(\tilde{\Delta})}} - 1 \right) \tau_{\max}.$$

Let $\tilde{\mathcal{A}}$ denote the product $\tilde{A}_{m\tilde{\Delta}+\tilde{\Delta}-1}\tilde{A}_{m\tilde{\Delta}+\tilde{\Delta}-2}\dots\tilde{A}_{m\tilde{\Delta}}$. Applying equation (5.12) recursively $\tilde{\Delta}$ times to calculate $x^{m\tilde{\Delta}+\tilde{\Delta}}$ from $x^{\tilde{\Delta}}$ yields:

$$\begin{aligned} x^{m\tilde{\Delta}+\tilde{\Delta}} &= \tilde{A}_{m\tilde{\Delta}+\tilde{\Delta}-1}\tilde{A}_{m\tilde{\Delta}+\tilde{\Delta}-2}\dots\tilde{A}_{m\tilde{\Delta}+1}x^{m\tilde{\Delta}+1} + \mathcal{X}^{m\tilde{\Delta}+\tilde{\Delta}} \\ &= \tilde{\mathcal{A}}x^{m\tilde{\Delta}+1} + \mathcal{X}^{m\tilde{\Delta}+\tilde{\Delta}}, \end{aligned} \tag{5.13}$$

where $\mathcal{X}^{m\tilde{\Delta}+\tilde{\Delta}}$ is the solution to the linear system (5.12) for $x^{m\tilde{\Delta}+\tilde{\Delta}}$ with $x^{m\tilde{\Delta}} = 0$ as the initial condition.

We note that since $\tilde{\mathcal{A}}$ is a product of row-stochastic matrices, $\tilde{\mathcal{A}}$ is row-stochastic

[2]. Using reasoning identical to that in the proof of Theorem 2, we conclude that:

$$\tilde{\mathcal{A}}_{kr} \geq \tilde{\eta} := \min \{h, 1 - h\}^b (1 - h)^{b(3(\delta - |\mathcal{E}| + d_{\max}) - 1)} \quad \text{for all } k \in \{1, \dots, N\}.$$

and therefore:

$$\max \left(\tilde{\mathcal{A}}x^{m\tilde{\Delta}} \right) \leq \tilde{\eta} x^{m\tilde{\Delta}} + (1 - \tilde{\eta}) \max \left(x^{m\tilde{\Delta}} \right) \quad (5.14)$$

and:

$$\min \left(\tilde{\mathcal{A}}x^{m\tilde{\Delta}} \right) \geq \tilde{\eta} x^{m\tilde{\Delta}} + (1 - \tilde{\eta}) \min \left(x^{m\tilde{\Delta}} \right). \quad (5.15)$$

From the definition of \tilde{B}_p , we see that all the disturbance terms in equation (5.12) are negative. Therefore:

$$\max \left(\mathcal{X}^{m\tilde{\Delta} + \tilde{\Delta}} \right) \leq 0. \quad (5.16)$$

From equation (5.11), substituting $y = m\tilde{\Delta}$ and $v = \tilde{\Delta}$, we obtain the following inequality:

$$\min \left(\mathcal{X}^{m\tilde{\Delta} + \tilde{\Delta}} \right) \geq - \left(1 - (1 - h)^{\mathcal{M}(\tilde{\Delta})} \right) \tau_{\max}. \quad (5.17)$$

Define $V : \mathbb{N} \rightarrow [0, 1[$ as $V(p) = \max(x^p) - \min(x^p)$. Equations (5.13) to (5.17) imply the following:

$$\begin{aligned} V \left(m\tilde{\Delta} + \tilde{\Delta} \right) &\leq \tilde{a} V \left(m\tilde{\Delta} \right) + \left(1 - (1 - h)^{\mathcal{M}(\tilde{\Delta})} \right) \tau_{\max}, \\ \implies \left(V \left(m\tilde{\Delta} + \tilde{\Delta} \right) - V_{\text{final}} \right) &\leq \tilde{a} \left(V \left(m\tilde{\Delta} \right) - V_{\text{final}} \right), \end{aligned} \quad (5.18)$$

where $\tilde{a} = 1 - \tilde{\eta}$ and $V_{\text{final}} = \frac{1}{\tilde{\eta}} \left(1 - (1 - h)^{\mathcal{M}(\tilde{\Delta})} \right) \tau_{\max}$.

Evaluating V_{final} , we see that **(A3)** implies that V_{final} is less than $\frac{1}{2} - l_0 - \tau_{\max}$. Since equation (5.18) implies that $V \left(m\tilde{\Delta} + \tilde{\Delta} \right)$ is a convex combination of V_{final} and

$V(m\tilde{\Delta})$ which are both less than $\frac{1}{2} - l_0 - \tau_{\max}$, we see that:

$$V(m\tilde{\Delta} + \tilde{\Delta}) < \frac{1}{2} - l_0 - \tau_{\max}. \quad (5.19)$$

Lastly, since $\phi(t) \in \Gamma(\frac{1}{2})$, like in the proof of Theorem 2, the arc length $V_{\text{arc-length}}(\phi(t))$ is simply given by $\max(\tilde{\phi}(t)) - \min(\tilde{\phi}(t))$. Therefore the arc length satisfies the following inequality: $V_{\text{arc-length}}(\phi(t_p)) \leq V(x^p)$, for all $p \in \mathbb{N}$, since x_p contains all the elements of $\tilde{\phi}(t_p)$. Equation (5.19) implies that $\phi(t_{m\tilde{\Delta} + \tilde{\Delta}}) \in \Gamma(\frac{1}{2} - l_0 - \tau_{\max})$.

Induction

All the previous steps of this proof are based on the assumption that the condition (5.2) is satisfied for $y = m\tilde{\Delta}$, and we have proved that if so, condition (5.2) is satisfied for $y = m\tilde{\Delta} + \tilde{\Delta}$. Since condition (5.2) is satisfied at $t = 0$, (which corresponds to $m = 1$) condition (5.2) must be satisfied for all $t \geq 0$ by induction. Hence all the previous steps of this proof are valid for $y = m\tilde{\Delta}$ for any $m \in \mathbb{N}$.

□

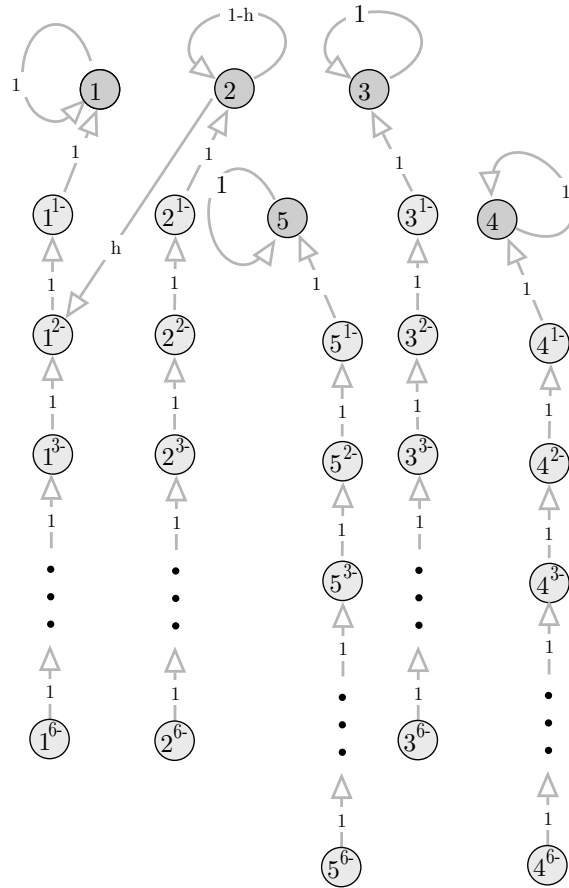


Figure 5.1: An example of a modified reception digraph $\tilde{\mathcal{G}}_p$, consistent with the reception digraph on the left in Figure 2.3, where oscillator 2 receives a pulse from oscillator 1 at t_p , and where two receptions have occurred in the duration $]t_p - \tau_{21}, t_p[$.

6 Examples and Numerical Simulations

PCO Network Examples Four example PCO networks that are not strongly connected but have a globally reachable node are simulated for randomly generated delays. The first three examples have a ‘star’ sensing digraph. The fourth example has an extra node added. The first and fourth examples have no delays and the second and third have delays. We expect the first and fourth examples to synchronize exactly, from the results of Section 4. In the second and third examples, we expect the system to approach synchrony, and the arc length function to converge to a non-zero value, from the results of Section 5.

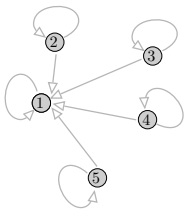
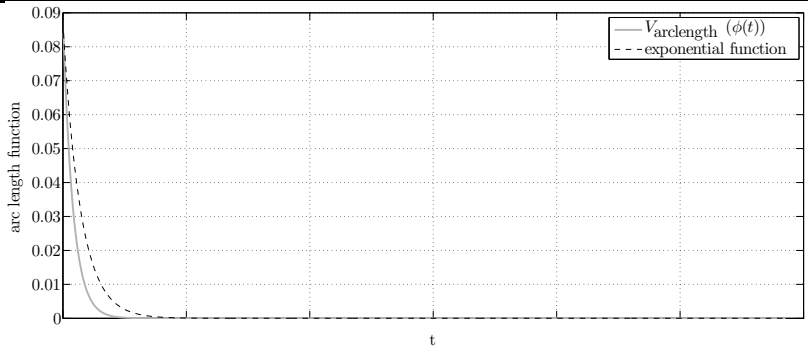
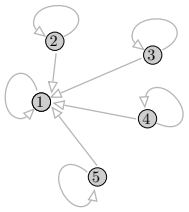
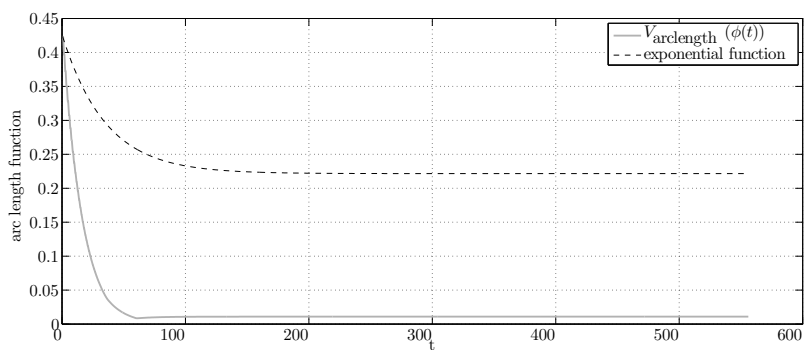
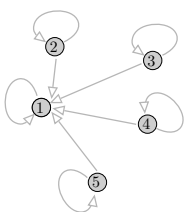
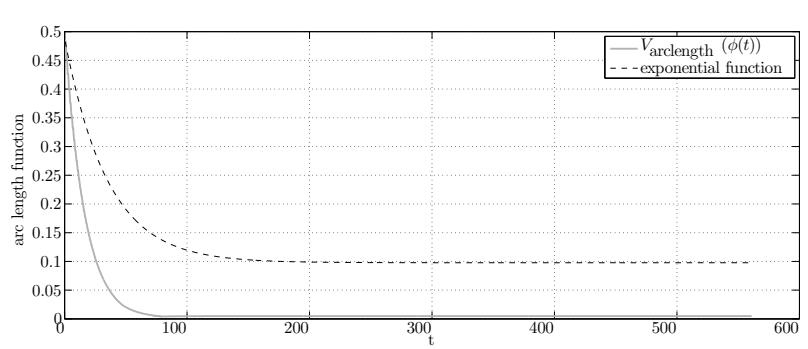
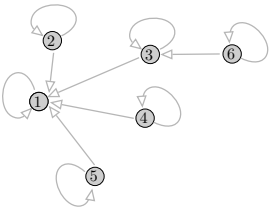
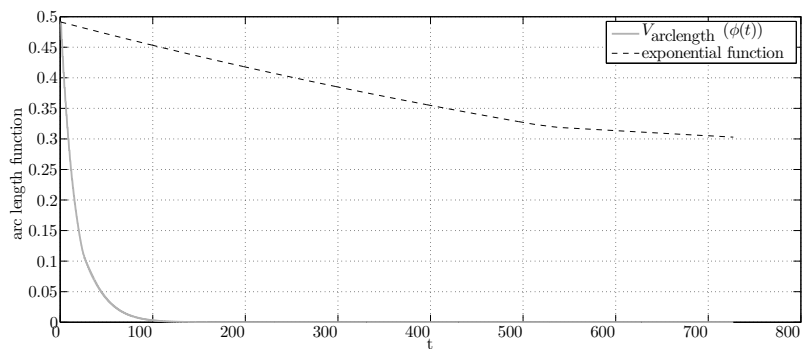
Simulation Model The simulation model was written in MATLAB and is included in Appendix A. The program first simulates the discrete dynamics. At each time step, the duration until the next discrete event (reset of any oscillator or reception of any pulse) is calculated. The state is then updated at the next time step by accounting for the continuous dynamics over this duration. The state vector consists of the phases of all the oscillators as well as states associated with pulses that have been sent but not yet received. The phases are then evaluated between the discrete events using the continuous dynamics. The arc length function is calculated from the phases, and plotted in Table 6.1.

Observations We make the following observations on the numerical results:

- The arc length function converges exponentially with the index m not the time t , so the shape of the time response may not appear exponential.
- For time indices that are not multiples of $\tilde{\Delta}$ the arc length function could remain constant or even increase by a finite amount, as seen in Figure 6.1.
- The final value of the arc length appears to increase with τ_{\max} .

- The arc length function is well within the predicted bounds, in fact, the bounds are quite weak for the examples. For networks with a larger number of nodes or a greater value of b (not pictured), the bounds are weaker still.
- Some simulations where the assumption **(A3)** was violated also converged to the predicted value, indicating that this assumption may be unnecessarily conservative.

Table 6.1: Example simulation results. All the simulations use $h = .06$.

	Sensing digraph	$V_{\text{arc-length}}$
1.		
	All τ_{ij} close to 0.	
2.		
	$\tau_{\max} = 0.0109$	
3.		
	$\tau_{\max} = 0.0048$	
4.		
	All τ_{ij} close to 0.	

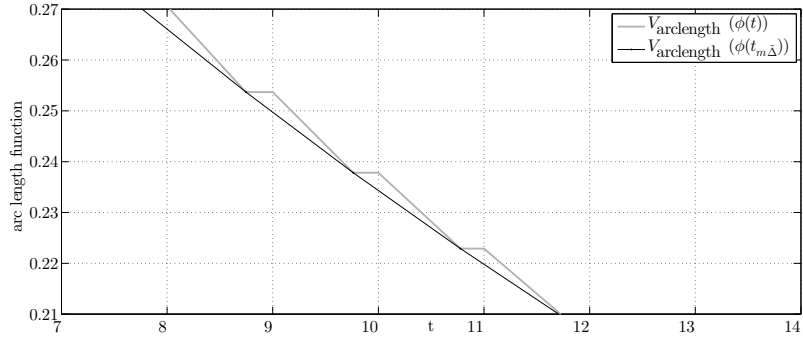


Figure 6.1: A magnification of the graph in Table 6.1 for example 2.

7 Conclusion

Remarks We developed a simple model to analyze PCO networks with mixed excitatory/inhibitory coupling in the presence of delays. We proved three theorems. Theorem 1 established bounds on the the times between firings of a given oscillator, and the time taken for a pulse to be received along every edge of the sensing digraph. Theorem 2 showed that if the sensing digraph has a globally reachable node, the pulse strength is sufficiently small, and no delays are present, then there exists a number Δ such that the arc length function converges exponentially over every Δ firings, for initial phases that are sufficiently close together. Theorem 3 showed that if the sensing digraph has a globally reachable node, the pulse strength is sufficiently small, and the delays are sufficiently small, then there exists a number $\tilde{\Delta}$ such that the arc length function converges exponentially over every $\tilde{\Delta}$ firings for initial phases that are sufficiently close together.

We also determined bounds on parameters including Δ , $\tilde{\Delta}$, the convergence rate, final value of arc length and the basin of attraction of the synchronized (or approximately synchronized solution) for a general sensing digraph. However, the method used in the proofs of the theorems may be repeated with specific knowledge of the sensing digraph for better bounds on the parameters.

In the analysis, we made the simplifying assumptions of equal pulse strengths on all edges, constant pulse strengths and constant delays. We estimated the rate of convergence and the basin of attraction of the solution. Numerical simulations bore out the analytical results qualitatively and quantitatively; however the quantitative bounds were weak. Also, convergence occurred even when the assumption **(A3)** was violated, which suggests that the assumption may be unnecessarily conservative.

Future Work Future work may attempt to find tighter bounds on the rate of convergence, the final value of the arc length function, and the basin of attraction.

Also, the model with constant pulse strength may be used as an approximation for PCO network systems where the coupling is nonlinear, that is, the phase jump depends nonlinearly on the phases. Also, the model may be extended to time-dependent delays. The applicability of the model to sensing digraphs that are not necessarily strongly connected but that instead satisfy the weaker condition of having a globally reachable node may enable improvements in technological applications, such as enabling clock synchronization in sensing and robotic networks to have weaker requirements on communication.

Appendix A: Simulation Program

The MATLAB program used to simulate the examples described in Section 6 is given below. It consists of the scripts `setup.m` and `run_sim.m`, and the functions `PCO_model.m`, `reception.m`, `M.m` and `Varclength.m` (`setup.m` is to be run first).

Script `setup.m`:

```
1 %define sys params:
2 global nnodes speeds incidence_matrix tol h delta nedges
   Tmax Tmin dmax
3 nnodes = 5; %number of nodes
4 tol = 2*eps;
5 h = 6e-2;
6
7 nruns = 5000; %length of simulation is till nruns discrete
   events
8 speedfac = 5e3; %magnitude of reciprocal of randomly
   generated delays.
9           %set to 5e14 to simulate no-delay case.
10 speeddiff = 5e-1; %variation in the reciprocals of the
   delays
11 yesdelay = 1; %1 if delays are present. If yesdelay == 0,
   set speedfac to 5e14
12
13
14 % generate the transpose of the binary adjacency matrix of
   the
15 % sensing digraph (excluding self-loops):
```

```

16
17 %% undirected ring graph
18 % Atransp= zeros(nnodes);
19 % Atransp(1,2) = 1; Atransp(1,end)=1;
20 % Atransp(end, nnodes-1) = 1; Atransp(end,1)=1;
21 % for ii = 2:nnodes-1;
22 %     Atransp(ii, ii-1:ii+1) = [1 0 1];
23 % end
24 % b = floor(nnodes/2);
25
26 %% Or,
27 %% directed ring graph
28 % Atransp = zeros(nnodes);
29 % Atransp(1,2) = 1; %Atransp(1,end)=1;
30 % Atransp(end,1)=1;
31 % for ii = 2:nnodes-1;
32 %     Atransp(ii, ii-1:ii+1) = [0 0 1];
33 % end
34 % b = nnodes-1;
35
36 %% Or,
37 %% undirected line graph
38 % Atransp= zeros(nnodes);
39 % Atransp(1,2) = 1;
40 % Atransp(end, nnodes-1) = 1;
41 % for ii = 2:nnodes-1;
42 %     Atransp(ii, ii-1:ii+1) = [1 0 1];

```

```

43 % end
44 % b = floor (nnodes / 2);
45
46
47 % Or,
48 % directed line graph
49 % Atransp= diag(ones (nnodes - 1, 1), 1);
50 % b = nnodes - 1;
51
52 % % Or,
53 % % a tree example
54 % nnodes = 5;
55 % Atransp = zeros (nnodes);
56 % Atransp (1, 2) = 1; Atransp (1, 3) = 1;
57 % Atransp (2, 4) = 1; Atransp (4, 5) = 1;
58 % b = 3;
59
60 % Or,
61 % a star example
62 nnodes = 5;
63 Atransp = zeros (nnodes);
64 Atransp (1, 2:end) = ones (nnodes - 1, 1);
65 b=1;
66
67 run_sim

```

Script run_sim.m:

```
1 %calculate # edges and PCO network params:
2 nedges = sum(sum(Atransp)); %number of edges
3 speeds = [ones(nnodes,1); speedfac*(1+speeddiff*rand(nedges
    ,1))];
4 taumax = max(1./speeds(nnodes+1:end));
5
6 %build incidence_matrix:
7 incidence_matrix = zeros(nnodes, nedges);
8 counter=1;
9 for ii = 1:nnodes
10     for jj = 1:nnodes
11         if Atransp(ii, jj)==1
12             incidence_matrix(ii, counter)=1;
13             incidence_matrix(jj, counter)=-1;
14             counter=counter+1;
15         end
16     end
17 end
18
19 %calculate quantities of interest
20 dmax = max(sum(Atransp,1));
21 Tmax = 1/2 + 1/(1-h*dmax)
22 Tmin = 1/2;
23 deltamax = 1+(nedges-1)*ceil(Tmax/Tmin);
24 delta = deltamax;
25 Delta = b*(delta + yesdelay*nedges);
```

```

26 MDelta = M(Delta);
27 eta = min([h 1-h])^b*(1-h)^(b*(3*(delta + dmax - nedges)-1));
28 a = 1-eta;
29 assumption3_lhs = taumax/eta*(1-(1-h)^MDelta) + taumax
    *(1-(1-h)^MDelta);
30 if assumption3_lhs >= 0.5
31     display('Error: Assumption 3 violated.')
32     pause()
33     return
34 end
35 Vf = taumax/(1-a)*(1 - (1-h)^MDelta);
36 l0 = (1/(1-h)^MDelta - 1)*taumax;
37 maxu = (1 - (1-h)^MDelta)*taumax;
38 %

```

```

39
40 %set up simulation
41 xlen = nnodes + nedges;
42 xi = [(0.5 - taumax - l0)*rand(nnodes, 1); 1e12*ones(nedges, 1)];
43 xi(1) = .0001; x(2) = 1/2 - l0 - taumax - eps;
44 xs = zeros(xlen, nruns);
45 deltats = zeros(1, nruns);
46 qs = zeros(1, nruns);
47
48 %run simulation:
49 x = xi;

```



```

50 for ii = 1:nruns
51     [deltats(ii) xs(:,ii) qs(ii)] = PCO_model(x);
52     x = xs(:,ii);
53     if max(x(1:nnodes))>1
54         return;
55     end
56
57     if deltats(ii) < tol
58         break
59     end
60 end
61 if ii < nruns
62     xs(:,ii+1:end) = [];
63     qs(:,ii+1:end) = [];
64     deltats(:,ii+1:end) = [];
65     nruns = ii;
66 end
67
68 %process output:
69 ts = cumsum(deltats); %times of discontinuity
70 tt = 0:0.005:ts(end); %'continuous' time, for interpolation
71 ttlen = length(tt);
72 phit = zeros(nnodes,ttlen); %phases in 'continuous' time
73 counter = 1;
74 phis = xs(1:nnodes,:);
75
76 phiprev = xi(1:nnodes);

```

```

77 tprev = 0;
78 for ii = 1:nruns-1
79     while tt(counter)<ts(ii)
80         if counter>=ttlen
81             break
82         end
83         phit(:,counter) = phiprev + (tt(counter)-tprev)*
            speeds(1:nnodes);
84         counter = counter+1;
85         if counter>=ttlen
86             break
87         end
88     end
89     tprev = ts(ii);
90     phiprev = xs(1:nnodes, ii);
91 end
92 tt = [tt ts]; phit = [phit xs(1:nnodes,:)];
93 [tt, iis] = sort(tt); phit = phit(:, iis);
94
95 Varlengths = zeros(1,length(ts));
96 for ii = 1:length(ts)
97     Varlengths(ii) = Varlength(phit(:, ii));
98 end
99
100 Varlengtht = zeros(1,length(tt));
101 for ii = 1:length(tt)
102     Varlengtht(ii) = Varlength(phit(:, ii));

```

```

103 end
104
105
106 iip = find(qs(:) == 1);
107 Varlengthp = Varlengths(iip);
108 tp = ts(iip);
109 VarlengthmDelta = Varlengthp(1:nnodes:end);
110 tmDelta = tp(1:nnodes:end);
111
112 VmDelta = zeros(1, length(tmDelta));
113 for ii = 1: length(tmDelta)
114     VmDelta(ii) = Vf + (Varlengtht(1)-Vf)*a^(ii-1);
115 end
116
117 figure
118 plot(tt, Varlengtht, 'g-', tt, Vf+0*tt, 'k-')
119 hold on
120 plot(tmDelta, VarlengthmDelta, 'k-', 'linewidth', 2)
121 plot(tmDelta, VmDelta, 'k-')
122 xlabel('t')
123 ylabel('V_{max-min}')
124 legend('arc length', 'arc length at sample times', 'V_{final}',
        , 'exponential function')

```

Function PCO_model.m:

```

1 function [deltat, ynew, q] = PCO_model(yold)
2 global nnodes speeds incidence_matrix tol

```

```

3 %column of incidence_matrix corresponds to an edge
4 %Eps is a vector of length = # edges
5 % phiold = xold(1:nnodes);
6 % etaold = xold(nnodes+1:end)
7
8 %find out when and what happens
9 deltats = (1-yold)./speeds;
10 temp2 = find(deltats(:)>0);
11 deltat = min(deltats(temp2));
12 iis = find((deltats(temp2(:))-deltat)<tol);
13 iis = temp2(iis);
14 if isempty(deltat)
15     deltat = 0;
16     iis = find(deltats(:)==0);
17 end
18 % ii = iis(temp2);
19
20
21 %first apply the drift
22 ynew = yold + speeds*deltat;
23
24 for jj = 1:length(iis)
25     ii = iis(jj);
26     if ii<=nnodes
27         q = 1; %fire
28     else
29         q = 0; %receive

```

```

30         ii = ii - nnodes;
31     end
32
33     %then apply discontinuous part (firing or receiving)
34     if q==1 %fire
35         temp = incidence_matrix(ii,:)'; %row corresponding
36             to firing node
37         temp = heaviside(temp).*temp; %1's where positive
38         %set elements of eta corresponding to the
39         %ones in temp to 0, leave others unchanged
40         ynew = ynew - [zeros(nnodes,1); temp].*ynew;
41         ynew(ii) = 0; %fired hence resets
42     else %receive
43         temp = incidence_matrix(:,ii); %col. corresponding
44             to received edge
45         temp = -heaviside(-temp).*temp; %1's where negative
46         %update elements of phi corresponding to -1 with
47         %jump function
48         ynew(1:nnodes) = reception(ynew(1:nnodes),temp);
49         ynew(nnodes+ii)=1; %just received, ensure exactly 1
50     end
51 end

```

Function reception.m:

```

1 function ynew = reception(y, pulsevec)
2 global h
3 ynew = y + h*(heaviside(y-1/2) - y).*pulsevec;

```

```
4 end
```

Function M.m:

```
1 function y = M(xin)
2 global delta nedges dmax
3 y = floor(xin/delta)*(delta-nedges+dmax) + min([mod(xin,
    delta) (delta-nedges+dmax)]);
4 end
```

Function Varclength.m:

```
1 function Vout = Varclength(phi)
2 %Since we will chose phi to remain within an arc of length
    half, the arc
3 %length function is the maximum pair-wise geodesic distance.
4 n = length(phi);
5 pairwise_distances = zeros(n,n);
6 for ii = 1:n
7     for jj = 1:n-1
8         pairwise_distances(ii , jj) = min(abs(phi(ii)-phi(jj)
            ),1-abs(phi(ii)-phi(jj)));
9     end
10 end
11
12 Vout = max(max(pairwise_distances));
```

Bibliography

- [1] J. Buck and E. Buck. Mechanism of rhythmic synchronous flashing of fireflies of Southeast Asia may use anticipatory time-measuring in synchronizing their flashing. *Science*, 159(3821):1319–1327, 1968.
- [2] F. Bullo. Lectures on network systems. Unpublished, June 2015.
- [3] C. C. Canavier and S. Achuthan. Pulse coupled oscillators and the phase resetting curve. *Mathematical Biosciences*, 226(2):77–96, 2010.
- [4] A. L. Christensen, R. O’Grady, and M. Dorigo. From fireflies to fault-tolerant swarms of robots. *IEEE Transactions on Evolutionary Computation*, 13(4):754–766, 2009.
- [5] J. P. Davis. The emergence and coordination of synchrony in organizational ecosystems. *Advances in Strategic Management*, 30:197–237, 2013.
- [6] K. Deng and Z. Liu. Distributed computation of averages over wireless sensor networks through synchronization of data-encoded pulse-coupled oscillators. *International Journal of Wireless Information Networks*, 16(1-2):51–58, 2009.
- [7] W. Gerstner. Rapid phase locking in systems of pulse-coupled oscillators with delays. *Physical Review Letters*, 76(10):1755, 1996.
- [8] Y. P. Hong, A. Scaglione, and R. Pagliari. Pulse coupled oscillators’ primitive for low complexity scheduling. In *IEEE Int. Conf. on Acoustics, Speech and Signal Processing*, pages 2753–2756, Taipei, Taiwan, Apr. 2009.
- [9] Y.-W. Hong and A. Scaglione. Distributed change detection in large scale sensor networks through the synchronization of pulse-coupled oscillators. In *IEEE Int. Conf. on Acoustics, Speech and Signal Processing*, volume 3, pages 869–872, May 2004.
- [10] Y. W. Hong and A. Scaglione. A scalable synchronization protocol for large scale sensor networks and its applications. *IEEE Journal on Selected Areas in Communications*, 23(5):1085–1099, 2005.
- [11] B. B. II, J. Kakalios, D. Nykamp, and T. I. Netoff. Dynamical changes in neurons during seizures determine tonic to clonic shift. *Journal of Computational Neuroscience*, 33(1):41–51, 2012.
- [12] D. Z. Jin. Fast convergence of spike sequences to periodic patterns in recurrent networks. *Physical Review Letters*, 89(20):208102, 2002.
- [13] J. Klinglmayr and C. Bettstetter. Synchronization of inhibitory pulse-coupled oscillators in delayed random and line networks. In *Int. Symposium on Applied Sciences in Biomedical and Communication Technologies*, pages 1–5, Rome, Italy, Nov. 2010.

- [14] J. Klinglmayr and C. Bettstetter. Self-organizing synchronization with inhibitory-coupled oscillators: Convergence and robustness. *ACM Transactions on Autonomous and Adaptive Systems*, 7(3):30, 2012.
- [15] Y. Kuramoto. Collective synchronization of pulse-coupled oscillators and excitable units. *Physica D: Nonlinear Phenomena*, 50(1):15–30, 1991.
- [16] A. Mauroy, P. Sacré, and R. J. Sepulchre. Kick synchronization versus diffusive synchronization. In *IEEE Conf. on Decision and Control*, pages 7171–7183, Maui, HI, USA, Dec. 2012.
- [17] R. E. Mirollo and S. H. Strogatz. Synchronization of pulse-coupled biological oscillators. *SIAM Journal on Applied Mathematics*, 50(6):1645–1662, 1990.
- [18] F. Núñez, Y. Wang, and F. J. Doyle. Increasing sync rate of pulse-coupled oscillators via phase response function design: theory and application to wireless networks. *IEEE Transactions on Control Systems Technology*, 21(4):1455–1462, 2013.
- [19] F. Núñez, Y. Wang, and F. J. Doyle. Global synchronization of pulse-coupled oscillators interacting on cycle graphs. *Automatica*, 52:202–209, 2015.
- [20] F. Núñez, Y. Wang, and F. J. Doyle. Synchronization of pulse-coupled oscillators on (strongly) connected graphs. *IEEE Transactions on Automatic Control*, 60(6):1710–1715, 2015.
- [21] C. S. Peskin. *Mathematical Aspects of Heart Physiology*. Courant Institute of Mathematical Sciences, 1975.
- [22] F. Silva, L. Correia, and A. L. Christensen. Modelling synchronisation in multi-robot systems with cellular automata: Analysis of update methods and topology perturbations. In *Robots and Lattice Automata*, pages 267–293. Springer, 2015.
- [23] Y. Taniguchi, G. Hasegawa, and H. Nakano. Self-organizing transmission scheduling mechanisms using a pulse-coupled oscillator model for wireless sensor networks. In *Int. Conf. on Digital Information Processing and Communications*, pages 84–89, July 2012.
- [24] M. Timme, T. Geisel, and F. Wolf. Speed of synchronization in complex networks of neural oscillators: analytic results based on random matrix theory. *Chaos: An Interdisciplinary Journal of Nonlinear Science*, 16(1):015108, 2006.
- [25] M. Timme and F. Wolf. The simplest problem in the collective dynamics of neural networks: is synchrony stable? *Nonlinearity*, 21(7):1579, 2008.
- [26] M. Timme, F. Wolf, and T. Geisel. Coexistence of regular and irregular dynamics in complex networks of pulse-coupled oscillators. *Physical Review Letters*, 89(25):258701, 2002.

- [27] A. Tyrrell and G. Auer. Decentralized slot synchronization for cellular mobile radio. *NTT DoCoMo Technical Journal*, 10:56–44, 2008.
- [28] N. Wakamiya and M. Murata. Scalable and robust scheme for data fusion in sensor networks. In A. J. Ijspeert, M. Murata, and N. Wakamiya, editors, *Biologically Inspired Approaches to Advanced Information Technology: First International Workshop, BioADIT 2004*, volume 3141 of *Lecture Notes in Computer Science*, pages 112–127. Springer, 2004.
- [29] W. Wu and T. Chen. Impossibility of asymptotic synchronization for pulse-coupled oscillators with delayed excitatory coupling. *International Journal of Neural Systems*, 19(06):425–435, 2009.
- [30] C. Zhu, S. Zhang, A. Dammann, S. Sand, P. Henkel, and C. Gunther. Return-to-base navigation of robotic swarms in Mars exploration using DoA estimation. In *Int. Symposium ELMAR*, pages 349–352, Zadar, Croatia, Sept. 2013.